Model-based left ventricle segmentation in 3D ultrasound using phase image

Chunliang Wang and Örjan Smedby

Center for Medical Imaging Science and Visualization (CMIV), Department of Medical and Health Sciences (IMH), Linköping University, SE-58185 Linköping, Sweden
{chunliang.wang, orjan.smedby}@liu.se

Abstract. In this paper, we propose a semi-automatic method for left ventricle segmentation. The proposed method utilizes a multi-scale quadrature filter method to enhance the 3D volume, followed by a model-based level set method to segment the endocardial surface of the left ventricle. The phase map from the quadrature filters is also used to weight the influence of contour points when updating the statistical model.

Keywords: left ventricle segmentation, model based level set method, quadrature filter, phase image

1 Introduction:

Three-dimension ultrasound (US) imaging is a relatively new method for analyzing cardiac function. Compared with other 3D modalities, such as CT and MRI, US is more available outside radiology departments and more cost-effective. However, a drawback of US imaging is the inferior image quality compared to CT or MRI, which makes it difficult to perform automated structure segmentation in US images. Numerous efforts have been made to improve the image quality and segmentation accuracy. Relatively complete reviews of the field can be found in [1], [2]. Local phase has been used as a robust image feature in noisy images in many US image segmentation applications [3], [4]. However, most existing methods perform the local phase estimation on a single scale, which limits the local phase to only reflect structures with a certain size. In practice, this means the local phase map is only valid within a limited distance from the edges. When combined with a segmentation method, such as active contours, the initial seed region has to be relatively close to the object border to benefit from the phase information. In this paper, we propose a semi-automatic method for left ventricle (LV) segmentation, which utilizes a multi-scale quadrature filter method [5] to enhance the 3D volume, followed by a model-based level set method to segment the LV endocardial surface. The integration of multi-scale filter output makes it easier to tell whether a point is inside or outside an object, even if the point is far away from the object border. In addition, the integrated multi-scale phase map is used to weight the model fitting process so that points far from edge will have less influ-

ence than points close to a clear edge. The proposed method delivered encouraging results on a small number of test datasets.

2 Method:

2.1 Image enhancement using 3D multi-scale quadrature filter

As most 3D US images are very noisy, an image enhancement step using 3D multi-scale quadrature filter was introduced as a preprocessing step. Quadrature filters, originally proposed by Granlund and Knutsson [6], have been successfully applied for various local structure estimation and image enhancement tasks [7]–[9]. The principle of these filters is to combine a ridge-picking filter with an edge-picking filter. Typical 2-dimensional filter kernels are illustrated in Fig. 1a and Fig. 1b. The output of this pair of filters is represented by a complex number where the output of the ridge-picking filter is seen as the real part and the output of the edge-picking filter as the imaginary part. When applied to an image, the response of ridge-like structures will be dominantly real, while the response of edge-like structures will be dominantly imaginary. The argument of this complex number in the complex plan is referred to as the *local phase* [6], θ in Fig 1c. To detect structures with various orientations, the image is often filtered with a set of quadrature filter pairs (e.g. 4 pairs in 2D and 6 pairs in 3D as suggested in [6]). The responses can be integrated into a tensor representation [6] or by simply adding the complex numbers up to a response map Q as suggested in [5]. In this study, the latter approach was chosen. Before summing up the output of these quadrature filter pairs, a phase correction step, as reported in [5], was carried out to ensure the edge responses from filters with opposite directions will not cancel out each other. A single-scale quadrature filter is limited to pick up lines with a certain width that is controlled by the central frequency and bandwidth of filter. In this study, we use a 6-direction quadrature filter set with a central frequency of $\pi/2$ and bandwidth of 6 octaves. To be able to detect structures with varying size, multi-scale quadrature filters were proposed by Läthén et al., where the response maps from different scale are combined using the magnitude of the response at each scale as a weighting factor.

$$q = \frac{\sum_{i=1}^{N} |q_i|^{\beta} q_i}{\sum_{i=1}^{N} |q_i|^{\beta}} \tag{1}$$

Here N is the number of scales, q_i is the response map for each scale and β is a real number parameter that controls the scaling of the difference between $|q_i|$ when translated to weighting factors. In this study, β is set to be 1 by visually comparing the enhanced images with different parameter settings. Three scales are used, and the scale ratios are 4x, 8x and 16x respectively.

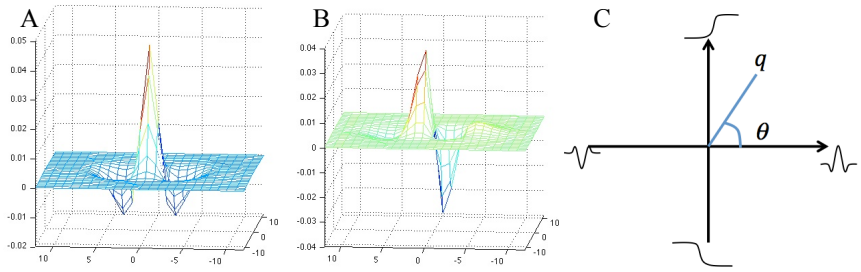

Fig. 1**.** An example of quadrature filter pairs in 2D. A, the ridge-picking filter. B, the edge-picking filter. C, The quadrature filter's response in the complex plane.

When applying the multi-scale quadrature filter on cardiac ultrasound images, the myocardial region has a positive real part due to its ridge-like (sheet-like in 3D) appearance, while the heart chambers have large negative real parts because they can be viewed as a dark line/dot at a large scale. In this study, we use the real part of the response map as an enhanced image for the remaining segmentation operations. An example of such enhanced images is shown in Fig 2B. A phase map Θ, which contains the arguments of all complex responses, is also created to guide the segmentation (explained in the next section).

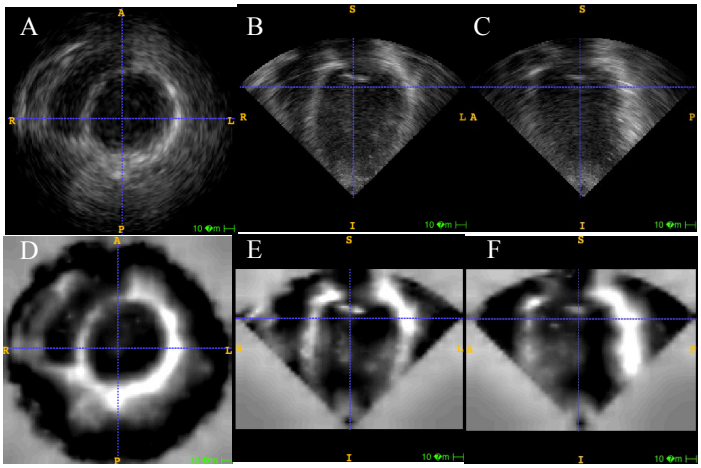

Fig. 2**.** An example of image enhancement using multi-scale quadrature filters. A, B, C, the axial, coronal and sagittal view of an input US image. D, E, F, the axial, coronal and sagittal view of the real part of the response map

2.2 Phase-map weighted model-based level set segmentation

In this study, the model-based level set method proposed by Leventon et al. [10] was adapted for endocardial surface segmentation. The principle of this method is to regularize the propagation of the level set function using a statistical shape model. This

model is also repeatedly updated using the current segmentation result. The speed function of the level set propagation is summarized in Eq. 2.

$$\frac{\partial \phi}{\partial t} = \alpha q_r \ + \mu \, \mathrm{M}(\mathrm{T}(x)) \ \ + \tau \, \kappa(x) \, |\nabla \Phi| \tag{2}$$

Here α, μ and τ are weighting factors. q_r is the real part of the multi-scale response map q. This term is similar to the threshold-based speed function, where the threshold is simply set to zero as the quadrature filter outputs negative real part inside the heart chambers and positive real part in myocardial area. $\kappa(x)$ represents the local curvature. $\mathrm{M}(\mathrm{T}(x))$ is the model term; the statistical shape model M can be written as the weighted sum of the mean signed distance functions ($\bar{M}$) and n prominent variations extracted via Principal Component Analysis (PCA) (M_1, M_2, … M_n) (Eq. 3). T is a rigid transform function with 7 parameters (3 for rotation, 3 for translation and 1 universal scaling factor).

$$\mathrm{M} = \bar{M} + \omega_1 M_1 + \omega_2 M_2 + \ldots + \omega_\mathrm{n} M_\mathrm{n} \tag{3}$$

To find the model most closely fitting the current level set function, we try to minimize the squared distance between M and ϕ_t, i.e. $\sum_{x \in Nar} (\mathrm{M}(\mathrm{T}(x)) - \phi_t(x))^2$, where Nar represents the narrow band around the zero level set. This least square problem can be solved by iteratively solving Eq. 4, i.e. using the Gauss–Newton algorithm. Here J is the Jacobian matrix of $\mathrm{M}(\mathrm{T}(x))$, $\Delta\rho$ is a n+7 parameter vector of the statistical model. Δy is the distance difference between the model and current level set function at point x. W is a diagonal weight matrix, whose elements control the influence of the sample points on the global parameter estimation. The design of W is explained below.

$$(\mathrm{J}^\mathrm{T}\mathrm{W}\mathrm{J})\Delta\rho = \mathrm{J}^\mathrm{T}\mathrm{W}\Delta y \tag{4}$$

A major challenge for LV segmentation in 3D US is missing signal around the apex area, where parts of the myocardium appear to be as dark as the heart chambers, or are left outside the field of view of the US beam (e.g. Fig. 2). This will cause the segmentation contour to leak outside of the LV. Another complication is the opening of the valves, which can also cause leakage of the contour. If the leaking area is large, it may eventually drive the model in the wrong direction. To overcome the erroneous influence of such leaking areas, we perform the model-fitting step using a weighting map, i.e. W in Eq. 4 created from the phase map Θ. The weighting factor for each point on the segmentation contour is computed using the following equation:

$$w_{ii} = sin^2(\theta(x_i)) + \gamma \tag{5}$$

Here γ is a non-negative real number which controls the relative weighting between voxels located in ridge-like structures and edge-like structures. If $\gamma = 0$, the voxels located far from edges (either bright or dark area in Fig. 2B) will have no influence on the model fitting. In practice, we set γ to 0.1 so that, when the initial level set function

is far from the object border, i.e. $sin^2(\theta)$ is close to zero, the model will still be updated.

To speed up the proposed segmentation method, a fast level set method using coherent propagation [11], [12] was implemented. It forces the whole segmentation contour to expand or shrink monotonically within a propagation period. The coherent propagation method can not only speed up the level set propagation, but also reduce the frequency of prior shape registration by taking advantage of the convergence detection of the coherent propagation [13], [14]. In this new framework, the model fitting operation is only repeated if the contour has moved a certain distance from the previously estimated model.

2.3 Model initialization using user input

To initialize the position of the statistical model, the user is requested to draw a line across the LV in one of the axial slices that is close to the center of the LV. The midpoint of this line is used to compute the translation from the model center. The length of the line is used to estimate the scaling transformation of the model. To tolerate possible operation errors by the human observer, the diameter of the model cross section is set to be 4/5 of the length of the input line, so that the model is always contained by the real LV (c.f. Fig. 3A). This line should also be pointed towards the right ventricle, which is used to calculate a rotation transformation around the z-axis. This line is merely used to initialize the LV model. It does not impose any constraint during the level set propagation.

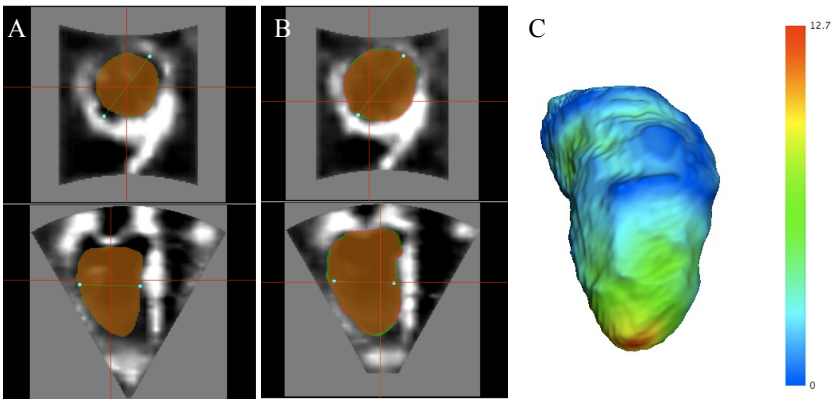

Fig. 3. A, Initialization of the statistical model (the green line was drawn by the user). B, Segmentation result. C, Error map.

3 Results:

The proposed algorithm was trained on 6 manually segmented LV by a medical expert from cardiac CT datasets that were collected for a coronary CTA study

[15](diastolic phase only). and tested on 15 training datasets and 15 testing datasets provided by the organizer of the challenge [16]. For comparison, the segmented regions were converted to 3D meshes using vtkContourFilter function from VTK library. Compared with the manually created references, the proposed method achieved a mean surface distance of 2.91 ± 1.13mm, mean Hausdorff surface distance of 13.21 ± 4.49mm and modified Dice similarity index of 0.16 ± 0.04. More detailed evaluation results are listed in Table 1 and 2. The overall running time of our C++ implementation was approximately 1-2 minutes on a PC with an Intel i7 CPU and 8Gb RAM.

Table 1. Segmentation accuracy on training datasets

Data group	Cardiac phase	MAD* (mm)	HD** (mm)	Modified DICE	Min error (mm)	Max error (mm)
Training data	End Diastolic	3.19	15.35	0.129	0.00	15.33
	End Systolic	3.46	14.60	0.163	0.00	14.60
Testing data	End Diastolic	2.86	13.20	0.147	0.00	13.02
	End Systolic	2.97	13.21	0.180	0.00	12.37

*: mean absolut distance

**:Hausdorff surface distance

Table 2. Segmentation accuracy on testing datasets

Data group	Statistics Terms	Participant End Diastolic Volume (ml)	Participant End Systolic Volume (ml)	Participant Ejection Fraction (%)	Participant Stroke Volume (ml)
Training data	Correlation	0.978	0.976	0.835	0.835
	Bias	-16.89	-18.25	3.95	3.95
	LOA*	[-84.4; 50.6]	[-67.4; 30.9]	[-12.5; 20.4]	[-12.57; 0.47]
Testing data	Correlation	0.813	0.871	0.862	0.519
	Bias	0.28	-4.83	3.17	5.11
	LOA*	[-69.69; 70.25]	[-57.13 ; 47.47]	[-7.14; 13.47]	[-19.54; 29.75]

*:limits of agreement

4 Discussion and Conclusion:

The proposed method yielded acceptable results for the test datasets provided. It is noticeable that the segmentation error of the proposed method is higher around the apex (Fig. 3C). This is explained by the missing signal of myocardium around the apex. Although using the weighting map helps to identify correctly the remaining parts of the LV, it cannot help to improve the segmentation accuracy in the missing parts.

In this study we used the real part of the quadrature filter set to guide the propagation of the level set function. To some extent, the real part of a quadrature filter can be seen as the second-order derivative of the intensity. The zero-crossing point of the

second-order derivative is well known as a good edge detector. However in single-scale settings, the second-order derivative may vanish inside the heart chamber where the first-order derivative is constantly zero. In such areas, the propagation of the contour has to be driven by a balloon force, which is designed to constantly inflate or deflate the region. This requires the initial seed region to be completely inside or outside the targeted object. By combining the multi-scale quadrature filter sets, the inside of LV and the myocardia will give negative and positive real parts, respectively. This eliminates the need for the balloon force and allows the initial seed region to be put partly inside and partly outside the LV.

The motivation to use models created from cardiac CT dataset instead of the provided "ground truth" for US datasets is that manual segmentation of US images is less reliable than that of CT images. As discussed above, in many US images, the signal around the apex area is very vague. Moreover, parts of the myocardium can be left outside the field of view of the US beam, whereas the endocardial surface is much clearer in CT images.

An obvious limitation of the presented work is that the statistical shape model was created on a small number of subjects using only end-diastolic images. Future work has been planned to improve the quality of the shape model by including more subjects with both systolic and diastolic phases.

Beside this limitation of the 3D model, the proposed method also ignores the connection between systolic and diastolic phases, and performs this two-phase segmentation as separated tasks. Linking them together, or considering the entire 4D sequence simultaneously, will hopefully lead to more accurate results. Adapting the 4D image denoising method developed by Eklund et. al. [9] may potentially improve the segmentation results. Another extension would be to use a 4D shape model instead of the 3D models. To reduce the complexity of the model representation, skeleton-based models proposed in [13], [17] may be used.

In conclusion, a model-based LV segmentation method using the phase image from quadrature filters is proposed. Preliminary results on 3D US images are encouraging.

5 Acknowledgement

We would like to thank Gunnar Läthén for publishing his Matlab code for multi-scale quadrature filter online [5].This research has been supported by the Swedish Research Council (VR), grant no. 2011-5197 and the Swedish Heart-Lung Foundation (HLF), grant no. 2011-0376.

6 References:

[1] S. H. Contreras Ortiz, T. Chiu, and M. D. Fox, "Ultrasound image enhancement: A review," *Biomedical Signal Processing and Control*, vol. 7, no. 5, pp. 419–428, Sep. 2012.

[2] J. Noble and D. Boukerroui, "Ultrasound image segmentation: a survey," *IEEE Transactions on Medical Imaging*, vol. 25, no. 8, pp. 987–1010, Aug. 2006.

[3] H. Knutsson and M. Andersson, “Morphons: segmentation using elastic canvas and paint on priors,” in *IEEE International Conference on Image Processing, 2005. ICIP 2005*, 2005, vol. 2, pp. II–1226–9.
[4] A. Belaid, D. Boukerroui, Y. Maingourd, and J.-F. Lerallut, “Phase-Based Level Set Segmentation of Ultrasound Images,” *IEEE Transactions on Information Technology in Biomedicine*, vol. 15, no. 1, pp. 138–147, Jan. 2011.
[5] G. Läthén, J. Jonasson, and M. Borga, “Blood vessel segmentation using multi-scale quadrature filtering,” *Pattern Recognition Letters*, vol. 31, no. 8, pp. 762–767, Jun. 2010.
[6] H. Knutsson, *Signal Processing for Computer Vision*. Springer, 1994.
[7] J. De Geer, M. Sandborg, Ö. Smedby, and A. Persson, “The efficacy of 2D, non-linear noise reduction filtering in cardiac imaging: a pilot study,” *Acta Radiol*, vol. 52, no. 7, pp. 716–722, Sep. 2011.
[8] Ö. Smedby, M. Fredrikson, J. De Geer, L. Borgen, and M. Sandborg, “Quantifying the potential for dose reduction with visual grading regression,” 2013.
[9] A. Eklund, M. Andersson, and H. Knutsson, “True 4D image denoising on the GPU,” *Journal of Biomedical Imaging*, vol. 2011, p. 8, 2011.
[10] M. E. Leventon, W. E. . Grimson, and O. Faugeras, “Statistical shape influence in geodesic active contours,” in *Computer Vision and Pattern Recognition, 2000. Proceedings. IEEE Conference on*, 2002, vol. 1, pp. 316–323.
[11] C. Wang, H. Frimmel, and Ö. Smedby, “Level-set based vessel segmentation accelerated with periodic monotonic speed function,” in *Proceedings of the SPIE Medical Imaging Conference*, 2011, p. 79621M–79621M–7.
[12] C. Wang, H. Frimmel, and Ö. Smedby, “Fast Level-set Based Image Segmentation Using Coherent Propagation,” *Med. Phys.*, vol. 41, no. 7, p. 073501, 2014.
[13] C. Wang and Ö. Smedby, “Fully automatic brain segmentation using model-guided level sets and skeleton-based models,” *The MIDAS Journal*, 2013.
[14] C. Wang and Ö. Smedby, “Automatic multi-organ segmentation in non-enhanced CT datasets using Hierarchical Shape Priors,” in *Proceedings of the 22th International Conference on Pattern Recognition (ICPR)*, Stockholm, 2014.
[15] C. Wang, A. Persson, J. Engvall, J. De Geer, W. Czekierda, A. Björkholm, S.-G. Fransson, and Ö. Smedby, “Can segmented 3D images be used for stenosis evaluation in coronary CT angiography?,” *Acta Radiol*, vol. 53, no. 8, pp. 845–851, Oct. 2012.
[16] “http://www.creatis.insa-lyon.fr/Challenge/CETUS/evaluation.html.” .
[17] C. Wang, R. Moreno, and Ö. Smedby, “Vessel segmentation using implicit model-guided level sets,” in *the 3D Cardiovascular Imaging: a MICCAI segmentation challenge workshop*, Nice, France, 2012.